J Solid State Electrochem (2012) 16:3189–3199
DOI 10.1007/s10008-012-1754-z

ORIGINAL PAPER

Graphene-carbon nanotubes modified graphite electrode for the determination of nicotinamide adenine dinucleotide and fabrication of alcohol biosensor

Simson Prasannakumar · Revanasiddappa Manjunatha · C. Nethravathi · Gurukar Shivappa Suresh · Micheal Rajamathi · Thimmappa Venkatarangaiah Venkatesha

Received: 29 January 2012 / Revised: 13 April 2012 / Accepted: 15 April 2012 / Published online: 9 May 2012

Abstract Through layer-by-layer adsorption (LBL) technique, the positively charged multiwalled carbon nanotubes (MWCNTs) and negatively charged graphene multilayer film were formed on graphite-poly(diallyldimethylammonium-chloride)-polystyrenesulphonate (Gr/PDDA/PSS) modified electrode. Due to large surface area and remarkable electrocatalytic properties of MWCNTs and graphene, the Gr/(PDDA/PSS-[MWCNTs-NH_3^+-graphene-COO^-]$_5$) electrode exhibits potent electrocatalytic activity towards the electrooxidation of nicotinamide adenine dinucleotide (NADH). A substantial decrease in the overpotential was observed at modified electrode, and the electrode showed high sensitivity to the electrocatalytic oxidation of NADH. The modified electrode was characterized by cyclic voltammetry and electrochemical impedance spectroscopy. The diffusion coefficient was calculated by chronocoulometry. Chronoamperometric studies showed the linear relationship between oxidation peak current and the concentration of NADH in the range 25–250 μM (R=0.999) with the detection limit of 0.1 μM (S/N=3). Further, dopamine, uric acid, acetaminophen and hydrogen peroxide do not interfere in the detection of NADH. The ability of MWCNTs and graphene to promote the electron transfer between NADH and the electrode exhibits a promising biocompatible platform for development of dehydrogenase-based amperometric biosensors. Alcohol dehydrogenase (ADH) was casted on Gr/(PDDA/PSS-[MWCNTs-NH_3^+-graphene-COO^-]$_5$) electrode; the resulting biosensor showed rapid and high sensitive amperometric response to ethanol with the detection limit of 10 μM (S/N=3).

Keywords Layer-by-layer technique · MWCNTs · Graphene · NADH · Alcohol dehydrogenase

S. Prasannakumar · R. Manjunatha · G. S. Suresh (✉)
Chemistry Research Centre, S. S. M. R. V. Degree College, Jayanagar,
Bangalore 560041, India
e-mail: sureshssmrv@yahoo.co.in

C. Nethravathi · M. Rajamathi
Materials Research Group, Department of Chemistry, St. Joseph's College,
36 Lalbagh Road,
Bangalore 560027, India

T. V. Venkatesha
Department of Chemistry, Kuvempu University, Jnanasahyadri,
Shimoga 577451, India

Introduction

Nicotinamide adenine dinucleotide plays a central role in mitochondrial respiratory metabolism by stimulating the energy production in all living cells. The detection of NADH is of great importance because it is produced in reactions that are catalyzed by hundreds of dehydrogenases. The electrochemical oxidation of NADH involves an electron transfer followed by deprotonation and a second electron transfer. The mechanism of the oxidation of NADH is reported to be as follows [1].

$$NADH - e^- \rightarrow NADH^{\cdot +} \quad (1)$$

$$NADH^{\cdot +} \rightarrow NAD^{\cdot} + H^+ \quad (2)$$

$$NAD^{\cdot} - e^- \rightarrow NAD^+ \quad (3)$$

The efficient recycling of NAD^+/NADH system is essential in the operation of a variety of electrochemical biosensors that are based on NAD^+-dependent dehydrogenase enzymes. The oxidation of NADH on unmodified electrodes suffers from high overpotential and form surface fouling due to the adsorption of radical intermediates produced [2]. The major product formed is NAD^+, which undergoes dimerization and gets adsorbed on the electrode surface hindering the direct electron transfer. Thus, the amperometric detection of NADH lacks stability and sensitivity. In addition, the electrochemical oxidation becomes unselective since at the high overpotential, other electroactive species present in the analyte solution would undergo oxidation.

The initial attempts to overcome these limitations were based on the use of redox mediators such as meldola blue [3, 4], prussian blue [5], phenoxazine [6], phenothiazine [7], toluidine [8] and quinones [9] to recycle the NADH back to the enzymatically active NAD^+. The activity of these mediators towards NADH oxidation has been explained in terms of hydride transfer mechanism in which the mediator accepts the hydride and has the ability to delocalize the electrons. Though such platforms offer an increased performance of the modified electrode for NADH sensing, there are still disadvantages such as leaching of mediators and the high overpotential that is not sufficient to eliminate interferences from other easily oxidizable species in real samples. The oxidation of NADH has been investigated using ferrocene [10, 11], conducting polymers [12–15] and nitrofluorenone derivatives [16, 17]. The recent approaches to facilitate the oxidation of NADH include the use of electrodes based on various forms of carbon such as pyrolytic graphite [18], carbon nanotubes (CNTs) [19–21] and graphene [22, 23].

CNTs are of great interest for the assembly of nanostructured macroscopic electrodes, biosensors and nano-bioelectronic devices due to their nanosize, lack of toxicity, good electrocatalytic properties and efficient accumulation of biomolecules as well as minimization of surface fouling. The unique properties of CNTs make them extremely attractive for the preparation of chemical sensors in general, particularly electrochemical sensors. In addition, CNTs can be functionalized with organic compounds with minimal change in their electronic and chemical properties.

Graphene, a 2-D, single layer sheet of sp^2 hybridized carbon atoms has attracted tremendous attention and research interest, owing to its exceptional physical properties, such as high electronic conductivity, good thermal stability and excellent mechanical strength. The promising properties together with the ease of processibility and functionalizability make graphene-based materials ideal candidates for the application in many areas including electrochemical sensing and biosensing. Graphene-based electrodes have been shown to exhibit excellent electron transfer promoting ability for some enzyme-based biosensors [24, 25].

Layer-by-layer (LBL) technique has been regularly employed in developing biosensors. Alternate adsorption of oppositely charged ions on solid electrode surface has been used to fabricate biosensors systems. Finely controlled multilayer films could be constructed using LBL method [26].

This paper demonstrates the construction of thin films of positively charged MWCNTs and negatively charged graphene on PDDA/PSS modified graphite electrode using LBL technique. The modified electrode decreases the overpotential for NADH oxidation and was used to develop an alcohol dehydrogenase based biosensor. The electrochemical behavior of the modified electrode towards determination of NADH was investigated by cyclic voltammetry, electrochemical impedance spectroscopy, chronoamperometry and chronocoulometry.

Experimental details

Reagents

NADH, multiwalled carbon nanotubes (MWCNTs), thionyl chloride, ethylenediamine, toluene, polystyrenesulphonate (PSS) (M_w 70,000), poly(diallyldimethylammoniumchloride) (PDDA) (M_w 200,000–350,000) and alcohol dehydrogenase were purchased from Sigma-Aldrich and used as received. Ethanol was received from Changshu Yangyuan Chemical, China. Phosphate buffer solution (PBS) was prepared using stock solutions of 0.1 M K_2HPO_4 and 0.1 M KH_2PO_4. The pH was adjusted using 0.1 M HCl and 0.1 M NaOH. All other chemicals used were of analytical grade, and they were used without further purification. All solutions were prepared with milli-*Q* water.

Electrochemical measurements

Cyclic voltammetry, chronoamperometry, chronocoulometry and electrochemical impedance spectroscopy were carried out with Versastat 3 (Princeton Applied Research, USA). All electrochemical measurements were carried out in a three-electrode electrochemical cell with Gr/(PDDA/PSS-[MWCNTs-NH_3^+-graphene-COO^-]$_5$) electrode as working electrode, saturated calomel (SCE) as reference electrode and platinum as auxiliary electrode.

Preparation of negatively charged graphene and positively charged MWCNTs

Graphene was produced by the solvothermal reduction of colloidal dispersions of graphite oxide according to the

procedure described in a research article [27]. In brief, about 1 g of graphite powder was added to 23 ml of cooled (0 °C) concentrated H_2SO_4, and about 3 g of $KMnO_4$ was added gradually with stirring and cooling, so that the temperature of the mixture was maintained below 20 °C. The temperature of the reaction mixture was increased to 35 °C and maintained for 30 min with constant stirring. To cause an increase in temperature to 98 °C, 46 ml of distilled water was slowly added, and the mixture was maintained at that temperature for 15 min. The reaction was terminated by adding 140 ml of distilled water followed by 10 ml of 30 % H_2O_2 solution. The solid product was separated by centrifugation and washed repeatedly with 5 % HCl solution until sulphate could not be detected with $BaCl_2$. Finally, the product was washed three to four times with acetone and dried in an air oven at 65 °C overnight. One hundred milligrams of graphene oxide was dispersed in 50 ml of ethylene glycol by sonication for 0.5 h at a temperature of 120 °C for 48 h. The brown colloidal dispersion was transferred to stainless steel autoclave, sealed and heated in oven. The graphene sheets obtained after solvothermal treatment were washed with acetone followed by water and then dried in hot air oven at 65 °C.

The conductivity of the graphene oxide (graphite oxide) is much lesser than that of reduced graphene oxide (graphene). Graphene oxide sheets were reduced to obtain high conductive graphene sheets. Graphene oxide showed a resistivity of about 188–413 kΩ/m [28]. However, resistivity decreases drastically to~15 kΩ/m after high thermal reduction with alcohol. Similarly electrical conductivity of graphene is 10,000-fold increased after reduction of graphene oxide [29]. Thus, we prepared graphene from graphene oxide by solvothermal reduction method. But it is difficult to get stable dispersion of graphene in aqueous media, because it aggregates in aqueous media and eventually precipitates. In order to overcome this, COO^- functional groups are introduced at the edges of graphene by refluxing with conc. HNO_3 for 5 h. The resulting functionalized graphene was well dispersed in water and does not aggregate. The presence of COO^- functional groups at graphene sheets was characterized by FT-IR and confirmed; the figure was given in our earlier research article [30].

MWCNTs were refluxed with H_2SO_4:HNO_3 (3:1 *v/v*) at 70 °C to obtain carboxylic acid functionalized MWCNTs (MWCNTs-COO^-) and then washed with distilled water and dried in vacuum at 50 °C. MWCNTs-COO^- was chlorinated by refluxing with thionyl chloride for 12 h. Amine functionalized MWCNTs (MWCNTs-NH_2) were obtained by reacting chlorinated MWCNTs with ethylene diamine in dehydrated toluene for 24 h at 70 °C. After washing with ethanol and distilled water several times, MWCNTs-NH_2 powder was dried at 50 °C in vacuum for 24 h [31].

Fabrication of Gr/(PDDA/PSS-[MWCNTs-NH_3^+-graphene-COO^-]$_5$) electrode

An electrode was made by inserting a graphite cylinder of 6-mm diameter in the hole of a Teflon bar with the same internal diameter. Electrical contact was made with a copper wire through the centre of the Teflon bar. Prior to the modification, the graphite electrode was polished to get a mirror shining surface using different grades of emery paper, i.e., 1000, 800, 6/0, 4/0 and finally with 2/0. It was than ultrasonicated for several minutes and rinsed with milli-*Q* water. Graphene-COO^- (2 mg/ml) was dispersed in pure water, and MWCNTs-NH_2 (2 mg/ml) was dispersed in acetate buffer (pH 3) to get MWCNTs-NH_3^+ [28]. The polished graphite electrode was dipped in PDDA (3 %*w/v*) containing 0.5 M NaCl for 1 h. The positively charged PDDA modified graphite electrode was immersed in PSS (3 % *w/v*) for 1 h to obtain negatively charged PDDA/PSS modified graphite electrode. This electrode was dipped alternately in MWCNTs-NH_3^+ and graphene-COO^- solution for 30 min each. The films were carefully rinsed in distilled water after each dipping step to remove excess and loosely held materials. The above procedure was repeated five times to obtain Gr/(PDDA/PSS-[MWCNTs-NH_3^+-graphene-COO^-]$_5$) electrode which is henceforth referred to as modified electrode.

Immobilization of enzyme on Gr/(PDDA/PSS-[MWCNTs-NH_3^+-graphene-COO^-]$_5$) electrode

Seven milligrams per milliliter of alcohol dehydrogenase (ADH) was dissolved in phosphate buffer solution at pH 7.0. Four microliters of enzyme was cast on to the modified electrode and dried at ambient temperature. The enzyme modified electrode was stored in phosphate buffer at pH 7.0 at 4 °C when not in use.

Results and discussion

Characterization of the Gr/(PDDA/PSS-[MWCNTs-NH_3^+-graphene-COO^-]$_5$) modified electrode using cyclic voltammetry and electrochemical impedance spectroscopy

The electrochemical behavior of bare graphite and modified electrodes in 0.1 M phosphate buffer solution is as shown in Fig. 1a. Well-defined peaks at 0.029 and −0.141 V were observed for the modified electrode due to the redox process of oxygen containing groups present in graphene-COO^- [20]. The cathodic and anodic peak currents increased linearly with increase in the number of bilayers [see inset in

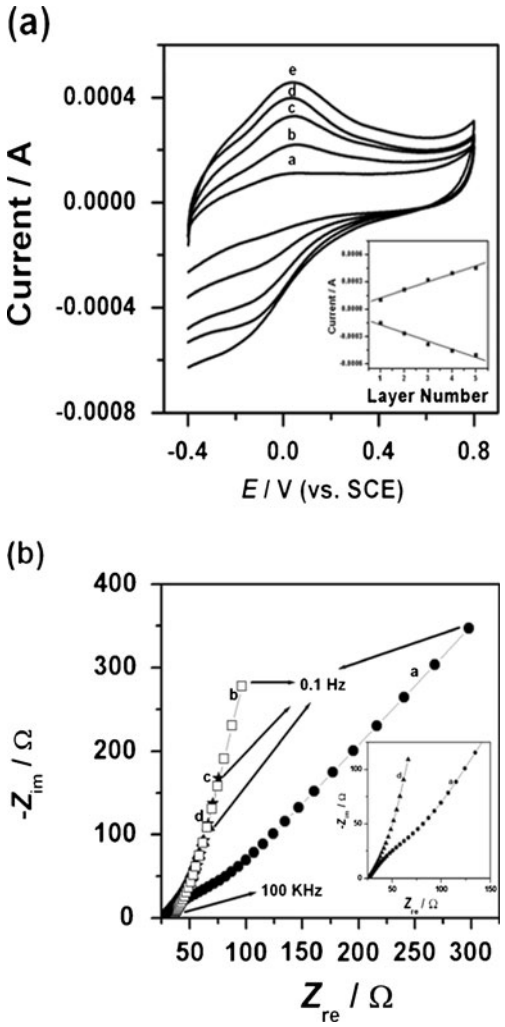

Fig. 1 Cyclic voltammograms of Gr/(PDDA/PSS-[MWCNTs-NH_3^+-graphene-COO^-]$_n$) modified electrode (**a**) where n=1–5 (*a*–*e*) in phosphate buffer solution of pH 7.0 at a scan rate of 0.05 Vs^{-1}; *a* is the cyclic voltammogram of bare electrode. **b** Nyquist impedance plots of bare (*a*), after first (*b*), third (*c*) and fifth (*d*) bilayer modification of the electrode in 1 mM $Fe(CN)_6^{4-/3-}$. The frequency range is from 100 kHz to 0.1 Hz, and amplitude is 5 mV. The supporting electrolyte is 0.1 M phosphate buffer containing 0.1 M KCl. *Inset* shows the charge transfer resistance of bare Gr (*a*) and fifth (*d*) bilayer

Fig. 1a], suggesting uniform growth of each bilayer. The linear equations were as follows:

$$i_{pa} = 3.71 \times 10^{-5} + 8.75 \times 10^{-5} N_L (R = 0.990) \quad (4)$$

$$i_{pc} = -8.02 \times 10^{-5} - 8.96 \times 10^{-5} N_L (R = 0.984) \quad (5)$$

where, N_L is the number of bilayers.

The modified electrode remained unaltered on continuous potential cycling and repetitive measurements, suggesting that the graphene-COO^- and the positively charged MWCNTs-NH_3^+ layers are bound strongly to each other through electrostatic interaction.

Electrochemical impedance spectroscopy is an effective method for probing the features of surface-modified electrodes using the redox probe $Fe(CN)_6^{4-/3-}$. Figure 1b shows that at bare graphite electrode the impedance spectrum was composed of a semicircle and a straight tail line. The semicircle part at high frequency corresponds to limited electron-transfer process, and the linear part at low frequency originates from the mass transfer limitation of $Fe(CN)_6^{4-/3-}$. Interestingly after modifying the graphite electrode with MWCNTs-NH_3^+ and graphene-COO^-, the semicircle was not observed and only a straight line was observed suggesting diffusion controlled electron transfer process. Because MWCNTs-NH_3^+ and graphene-COO^- are excellent electric conducting materials, they could accelerate the electron transfer and resulted in the reduction of charge transfer resistance [32]. This indicates that the impedance offered by modified electrode–electrolyte interface for charge transfer process is less compared to the bare electrode. Impedance decreases as the number of bilayers increases [33].

Morphology of MWCNTs and graphene modified electrode surfaces

The modified electrode is characterized by SEM. Figure 2 displays typical images of bare Gr (a), first bilayer (b), third bilayer (c) and fifth bilayer (d) of the modified electrode. The bare Gr electrode exhibits high heterogeneity with many cavities and stacked flakes. Upon modification with MWCNTs and graphene (first bilayer), the surface of the electrode shows decrease in cavities and stacked flakes. Similarly for the third and fifth bilayers, the adsorption of MWCNTs and graphene increases. Thus, one may expect to obtain a porous film of MWCNTs and graphene with a large surface area.

Electrocatalytic oxidation of NADH at Gr/(PDDA/PSS-[MWCNTs-NH_3^+-graphene-COO^-]$_5$) electrode

At unmodified carbon electrodes, the oxidation of NADH occurs at very high potential (> 0.7 V) with the surface fouling due to the accumulation of reaction intermediates (NAD^+) on the surface of the electrodes with many electrochemical interferences such as ascorbic acid, dopamine and uric acid [34, 35]. Cyclic voltammetric technique was used to determine the influence of bilayers on the electrocatalytic activity towards NADH. From Fig. 3a we observe that the oxidation of NADH on modified electrode occurs at +0.07 V. With increase in the number of bilayers, the oxidation current increases, and it remains almost constant after the formation of fifth bilayers. Hence, Gr/(PDDA/PSS-[MWCNTs-NH_3^+-graphene-COO^-]$_5$) electrode was used for further studies. Cyclic voltammograms recorded in

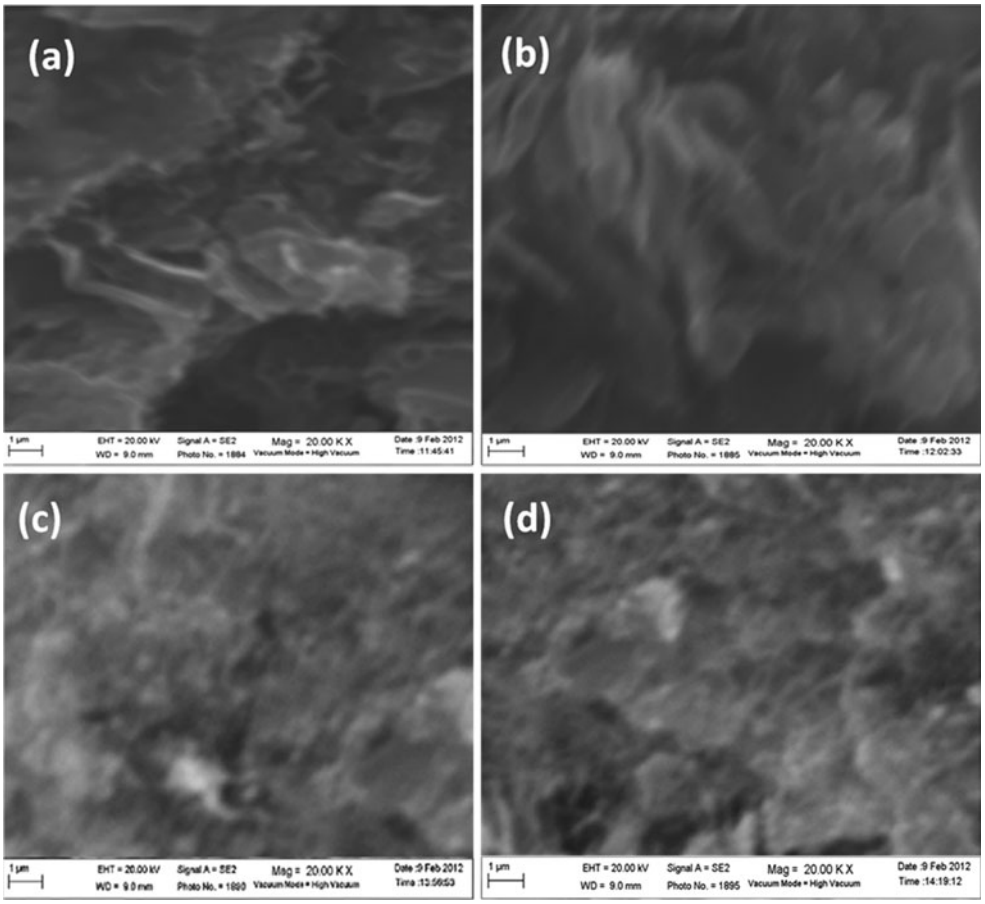

Fig. 2 SEM of bare Gr (**a**), first bilayer (**b**), third bilayer (**c**) and fifth bilayer (**d**) of MWCNTs and graphene

phosphate buffer (pH 7.0) for Gr/(PDDA/PSS-[MWCNTs-NH_3^+-graphene-COO^-]$_5$) electrode, in the absence and in the presence of 5 mM NADH, are shown in Fig. 3b. The modified electrode exhibits substantial negative shift of anodic peak potential (> 0.6 V) and high electrocatalytic activity for the oxidation of NADH. The large decrease in the overpotential and high electrocatalytic activity for the oxidation of NADH at the modified electrode is ascribed to the high surface area provided by MWCNTs and graphene.

Effect of increasing concentration and scan rate at Gr/(PDDA/PSS-[MWCNTs-NH_3^+-graphene-COO^-]$_5$) electrode

The cyclic voltammogram responses for a series of NADH solution with various concentrations are shown in Fig. 4a. With the addition of NADH, there was an increase in the anodic peak current linearly. In the limiting case, where all of the electroactive species undergoing a charge transfer is adsorbed at the solution–electrode interface, the peak current (i_p) will be proportional to scan rate (ν), and a plot of ln i_p vs ln ν will have a slope of 1. If a non-adsorbed electroactive species undergoes charge transfer either reversibly or irreversibly, a slope of ln i_p vs ln ν will be 0.5 [36]. Thus, for Gr/(PDDA/PSS-[MWCNTs-NH_3^+-graphene-COO^-]$_5$) electrode, a slope ln i_p vs ln ν was found to be 0.65. It depicts that oxidation of some adsorbed NADH is taking place at electrode surface. Thus, slight positive shift in peak potential with increase in concentration of NADH could be due to some amount of NADH adsorbed on electrode surface. The linear regression equation is given by

$$i_{p(NADH)}(A) = 4.28 \times 10^{-4} + 1.35 \times 10^{-5} C_{NADH}(mM),$$
$$R = 0.999,\ SD = 9.4 \times 10^{-7}. \quad (6)$$

Figure 4b shows the cyclic voltammograms recorded for 5 mM NADH solution in different scan rates. It is observed that by increasing the sweep rate, the peak potential for the oxidation of NADH shifts to more positive values. The peak currents for the anodic oxidation of NADH are proportional to the square root of scan rate, predicting a diffusion controlled process [37]. The inset in the figure shows the

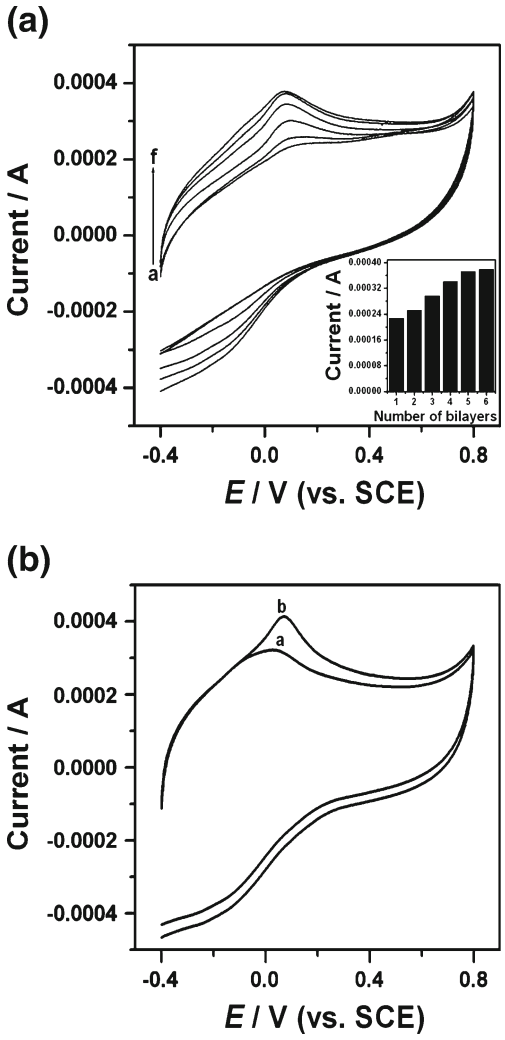

Fig. 3 Cyclic voltammograms of **a** [MWCNTs-NH_3^+-graphene-COO^-] bilayers on Gr/PDDA/PSS modified graphite electrode where n=1–6 (*a–f*) in phosphate buffer solution at pH 7.0 containing 0.1 M KCl and 5 mM NADH at a scan rate of 0.05 $V s^{-1}$. **b** Gr/(PDDA/PSS-[MWCNTs-NH_3^+-graphene-COO^-]$_5$) modified electrode in the absence (*a*) and presence (*b*) of 5 mM NADH

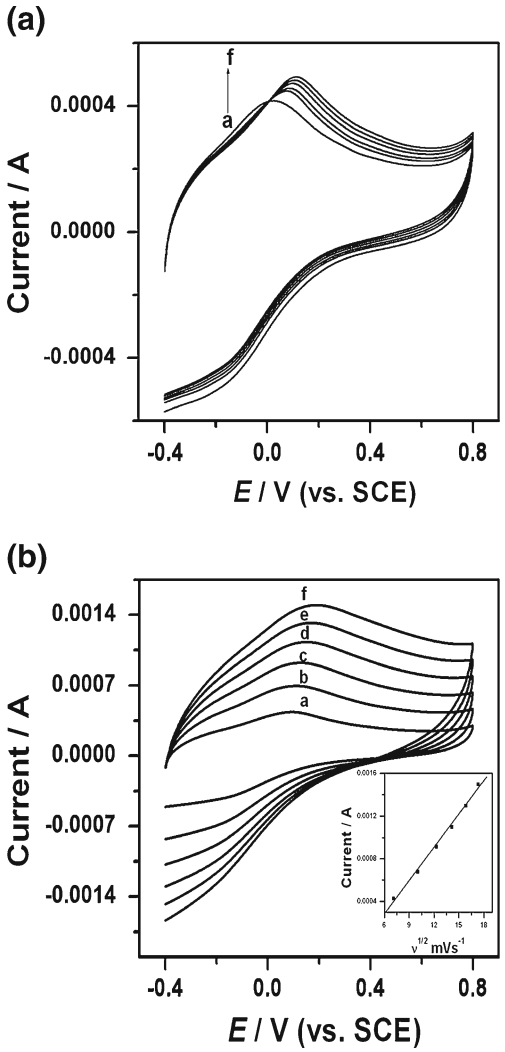

Fig. 4 Cyclic voltammograms of Gr/(PDDA/PSS-[MWCNTs-NH_3^+-graphene-COO^-]$_5$) **a** for varying NADH concentrations of 0, 1, 2, 3, 4 and 5 mM (*a–f*) in phosphate buffer solution at pH 7.0 containing 0.1 M KCl at a scan rate of 0.05 $V s^{-1}$. *Inset*: The calibration curve; (**b**) at different scan rates (*a–f*) of 0.05, 0.1, 0.15, 0.2, 0.25 and 0.3 $V s^{-1}$ in a solution containing 5 mM NADH. *Inset*: Plot of I_p vs (scan rate)$^{1/2}$

relation between scan rate and anodic peak current, and the linear regression equation is given by

$$i_p(\mathrm{A}) = -3.4 \times 10^{-4} + 1.0 \times 10^{-4} \nu\left(\mathrm{V\ s^{-1}}\right), \quad (7)$$

$$R = 0.997,\ \mathrm{SD} = 3.3 \times 10^{-5}$$

Adsorption of NADH on Gr/(PDDA/PSS-[MWCNTs-NH_3^+-graphene-COO^-]$_5$) electrode using chronocoulometry

The diffusion characteristics of NADH at the Gr/(PDDA/PSS-[MWCNTs-NH_3^+-graphene-COO^-]$_5$) electrode were investigated by chronocoulometry, according to the integrated Cottrell equation:

$$Q = 2nFAC(Dt)^{1/2}/\pi^{1/2} + Q_{dl} + Q_{ads} \quad (8)$$

where Q_{dl} is the double-layer charge and Q_{ads} is the Faradaic charge due to the oxidation of adsorbed NADH. Q_{ads} can be calculated from the difference of the intercepts of the plot of Q versus $t^{1/2}$ in the presence and absence of NADH. Q_{dl} is assumed not changed in the presence and absence of NADH [38, 39]. A is the surface area of the working electrode, C is the concentration of NADH, F is Faraday constant. Figure 5 shows the chronocoulometric curve obtained with modified electrode in the absence of NADH (curve a) and in the presence of 25 μM NADH at an applied potential of +0.07 V (curve b). The plot of Q has a linear relationship with the square root of time ($t^{1/2}$) (as shown in inset). The number of electrons involved in the oxidation of NADH is 2. A is 0.28 cm^2 and C is

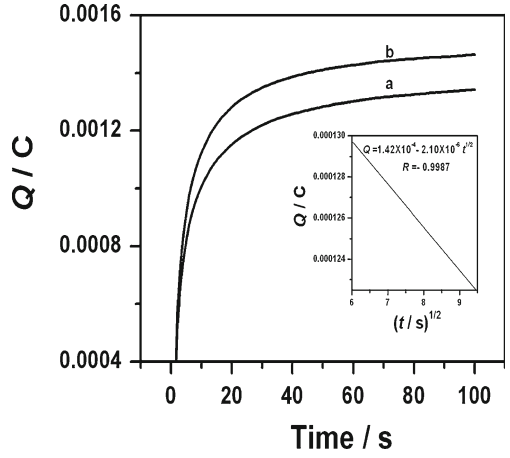

Fig. 5 Chronocoulometric curve of modified graphite electrode (*a*) in buffer solution and (*b*) for 25 μM NADH in phosphate buffer solution at pH 7. The *inset* shows the linear relationship between charge (*Q*) and square root of time ($t^{1/2}$)

2.5×10^{-5} mol L^{-1}. The calculated diffusion coefficient is 1.32×10^{-6} cm^2 s^{-1} from chronocoulometry, and the same is calculated from cyclic voltammetric method using the Randles–Sevcik equation:

$$i_p = \left(2.69 \times 10^5\right) n^{3/2} A C D^{1/2} \nu^{1/2} \quad (9)$$

and it is found to be 2.99×10^{-6} cm^2 s^{-1} (concentration of NADH used for the calculation is 5 mM). The value of the diffusion coefficient of NADH calculated is in good comparison with the values reported in literature, i.e., 2.4×10^{-6} cm^2 s^{-1} [12] and 2.98×10^{-6} cm^2 s^{-1} [15]. The surface coverage of the electrode was calculated by adopting the method due to Laviron [40]. According to this method, the total amount of charge (*Q*) is related to the surface concentration of electroactive species (Γ_s) by the equation

$$\Gamma_s = Q_{ads}/nFA \quad (10)$$

The surface coverage was found to be 2.75×10^{-9} mol cm^{-2}.

Constant amperometric determination of NADH at Gr/(PDDA/PSS-[MWCNTs-NH_3^+-graphene-COO^-]$_5$) electrode

Figure 6a shows the amperogram recorded for the Gr/(PDDA/PSS-[MWCNTs-NH_3^+-graphene-COO^-]$_5$) electrode at a working potential of +0.07 V with successive additions of NADH into the 0.1 M phosphate buffer solution at pH 7.0. The reaction occurring at the Gr/(PDDA/PSS-[MWCNTs-NH_3^+-graphene-COO^-]$_5$) electrode was very fast, reaching a dynamic equilibrium upon each addition of the analyte with a response time less than 3 s to reach 100 % signal. Such a fast amperometric response time is indicative

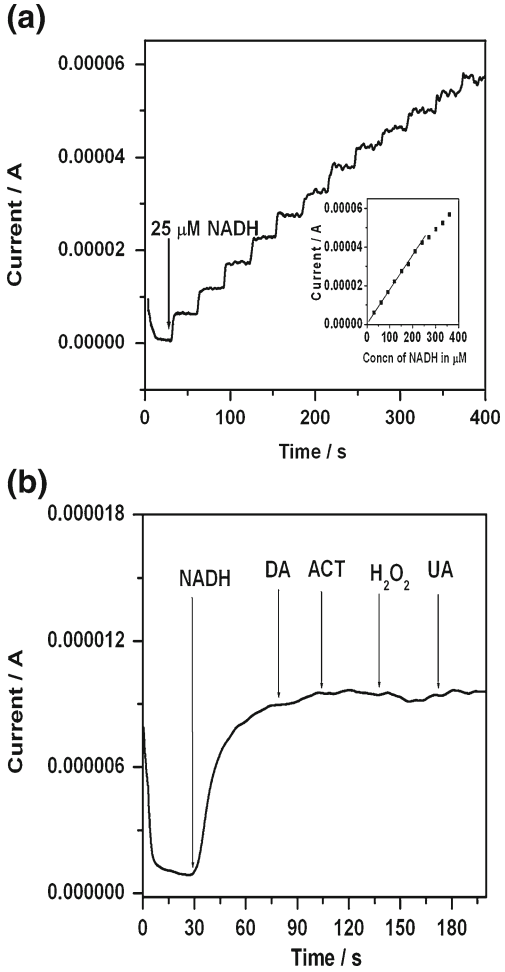

Fig. 6 Chronoamperometric response of Gr/(PDDA/PSS-[MWCNTs-NH_3^+-graphene-COO^-]$_5$) electrode for the oxidation of NADH at +0.07 V in phosphate buffer solution (pH 7.0). Each addition increased the concentration of NADH by 25 μM (**a**). *Inset*: plot of NADH vs. catalytic peak current. Amperometric response depicting the effect of coexisting DA, ACT, H_2O_2 and UA on the measurement of NADH at Gr/(PDDA/PSS-[MWCNTs-NH_3^+-graphene-COO^-]$_5$) (**b**) at the applied potential of +0.07 V in phosphate buffer solution at pH 7.0

of faster charge transport on the modified electrode. A wide linear response range from 25–250 μM was observed, and the linear regression equation is as follows:

$$i_{pNADH}(A) = 1.2 \times 10^{-6} + 1.7 \times 10^{-7} C_{NADH}(\mu M), \quad (11)$$

$$R = 0.999,\ SD = 5.4 \times 10^{-7}$$

A sensitivity of 55 μA cm^{-2} μM^{-1} was obtained. Various NADH sensors have been reported in literature. However, it is very difficult to compare one sensor to other because the performance of the sensor is greatly dependent on the applied potential, supporting electrolyte, electrode material and its surface area. Different NADH sensors are summarized in Table 1 with respect to operating conditions, sensitivity and the detection limit; it can be seen that the

Table 1 Comparison of the Gr/(PDDA/PSS-[MWCNTs-NH_3^+-graphene-COO^-]$_5$) electrode with other biosensors

NADH biosensor	Applied potential (V vs. SCE)	Sensitivity ($\mu A\ mM^{-1}\ cm^{-2}$)	Detection limit (μM)	Response time (s)	References
IL-graphene/chitosan/GC	+0.45	37	–	< 10	[23]
BCNS/GC	+0.3	2.25	0.05	–	[41]
TCBQ/MWCNTs/EPPG	+0.15	–	0.05	< 1	[21]
GCE/MWCNTs/poly-Xa	+0.1	2.2	0.1	< 0.1	[12]
CGA-modified carbon composite electrode	+0.3	0.025	0.2	< 1	[42]
Ti-MCM-41/GCE	+0.28	0.0018	8	–	[43]
BDD electrode	+0.58	–	0.01	–	[44]
Peptide nanotube-based gold electrode	+0.4	–	–	–	[45]
Catechin/PEDOT/GC	+0.35	0.019	0.5	–	[46]
Gr/(PDDA/PSS-[MWCNTs-NH_3^+-graphene-COO^-]$_5$) electrode	+0.07	55	0.1	< 3	Present work

performance of the developed sensor is comparable to most of NADH sensors in literature in one or more categories [41–46]. The detection and quantification limits were estimated at 0.1 μM (S/N=3) and 5 μM, respectively. We investigated the effect of interfering species commonly found in biological samples such as DA, UA, ACT and H_2O_2 as shown in Fig. 6b. The addition of NADH to the stirred solution shows the increasing current response; however, the addition of interfering species such as DA (50 μM), UA (50 μM), ACT (50 μM) and H_2O_2 (250 μM) did not show any current response. The prepared modified electrode is good for NADH sensor.

The effect of pH at Gr/(PDDA/PSS-[MWCNTs-NH_3^+-graphene-COO^-]$_5$) electrode towards oxidation of NADH

The effect of solution pH on the response of NADH at Gr/(PDDA/PSS-[MWCNTs-NH_3^+-graphene-COO^-]$_5$) electrode was investigated over the range of pH 4–8. Figure 7 shows that the anodic peak current and peak potential decrease with increase in pH. This shows that proton is involved in the oxidation of NADH. The maximum oxidation peak current was observed at pH 4.0. However, to mimic the physiological condition, pH 7.0 was chosen in this work.

Stability and reproducibility

Long-term stability is one of the most important requirements of biosensors. The stability of Gr/(PDDA/PSS-[MWCNTs-NH_3^+-graphene-COO^-]$_5$) electrode was checked in the presence of 0.5 mM NADH by performing amperometric experiment in 0.1 M phosphate buffer solution of pH 7.0 at an applied potential of +0.07 V under stirring condition for a period of 20 min. Figure 8 shows that the decrease of current observed was only around 10 % even in stirring condition indicating that the modified electrode is stable and suitable for sensor application. The modified electrode showed an

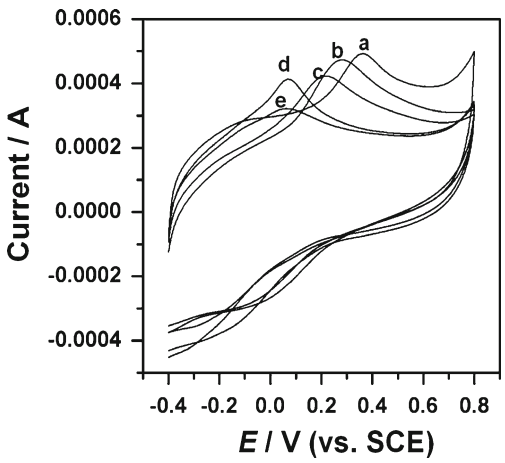

Fig. 7 Effect of pH at Gr/(PDDA/PSS-[MWCNTs-NH_3^+-graphene-COO^-]$_5$) on the cyclic voltammetric response of 5 mM NADH. pH (*a*) 4.0, (*b*) 5.0, (*c*) 6.0, (*d*) 7.0 and (*e*) 8.0

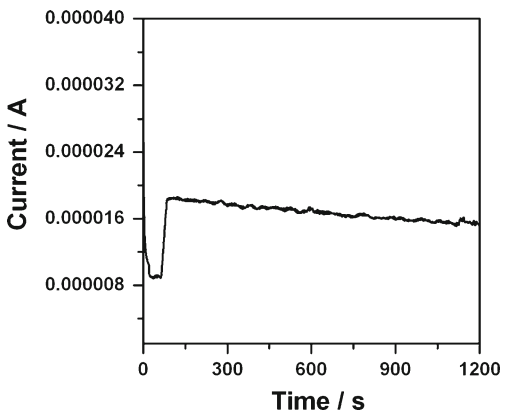

Fig. 8 Stability of the current response of 0.5 mM NADH at Gr/(PDDA/PSS-[MWCNTs-NH_3^+-graphene-COO^-]$_5$) at the applied potential of +0.07 V in phosphate buffer solution at pH 7.0

acceptable repeatability. The interface was prepared eight times in the same manner, and tests were performed in 0.1 M phosphate buffer at pH 7.0. A relative standard deviation lower than 5 % was obtained indicating good repeatability of the preparation of the sensor.

Effect of metal ions on the electrooxidation of NADH using Gr/(PDDA/PSS-[MWCNTs-NH_3^+-graphene-COO^-]$_5$) electrode

It is evident from Fig. 9a that the anodic current for the oxidation of NADH increases in the presence of metal ions.

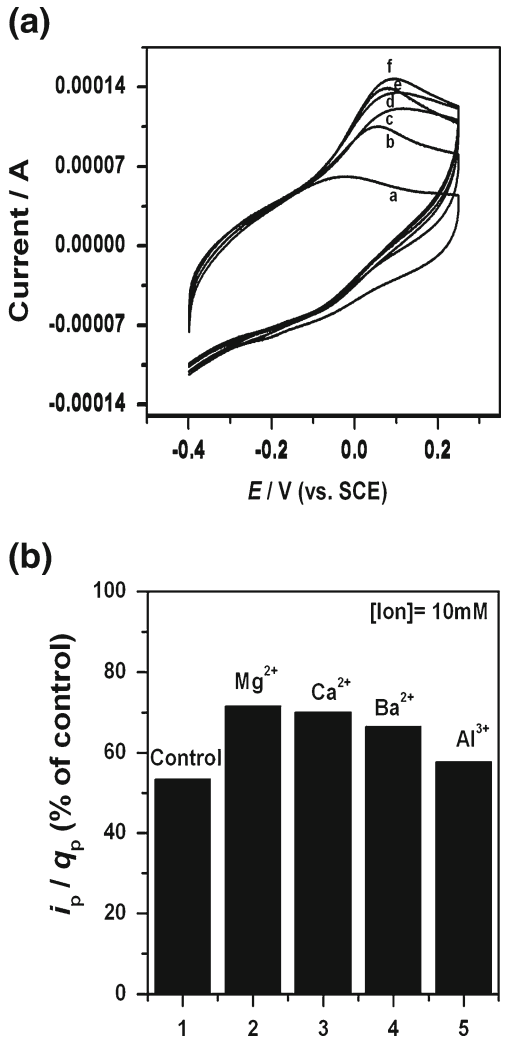

Fig. 9 Cyclic voltammograms at 0.01 Vs^{-1} of Gr/(PDDA/PSS-[MWCNTs-NH_3^+-graphene-COO^-]$_5$) electrode in 0.1 M phosphate buffer (pH7.0.) (*a*) and in the presence of 5 mM NADH (*b*), 5 mM NADH+10 mM $AlCl_3$ (*c*), 5 mM NADH+10 mM $BaCl_2$ (*d*), 5 mM NADH+10 mM $CaCl_2$ (*e*) and 5 mM NADH+10 mM $MgCl_2$ (**a**). Charge normalized peak currents (i_p/q_p) for the electroxidation of 5 mM NADH at Gr/(PDDA/PSS-[MWCNTs-NH_3^+-graphene-COO^-]$_5$) electrode in 0.1 M phosphate buffer (pH 7.0). The control represents the value obtained for the charge normalized peak current in the absence of added metal ions (**b**)

This may be due to the relationship between the presence of carboxylic groups (negative charge) on the electrode surface which binds between NADH and the catalyst due to the formation of metal ion bridge. Curves a and b in Fig. 9a show respective cyclic voltammograms at 0.01 Vs^{-1} of Gr/(PDDA/PSS-[MWCNTs-NH_3^+-graphene-COO^-]$_5$) electrode in phosphate buffer at pH 7.0 in the absence and presence of 5 mM NADH. Electrocatalytic oxidation of NADH varies with concentration of metal ions, and the maximum oxidation current was observed in the presence of 10 mM metal ions. Therefore, we have added specific amount (10 mM) of metal ions in to the solution. Curves c to f show the effects on the electrocatalytic current in the presence of 10 mM $AlCl_3$, $BaCl_2$, $CaCl_2$ and $MgCl_2$, respectively, in the solution. Ca^{2+} and Mg^{2+} ions enhanced the electrocatalytic current significantly for the oxidation of NADH. Other metal ions like Al^{3+} and Ba^{2+} show a similar behavior, but the effects are not as pronounced as in the case of Ca^{2+} and Mg^{2+} ions. In order to compare the results of the modified electrode in the absence and presence of different ions, the peak current was normalized to the charge of the modified electrode alone (i_p/q_p). This was then expressed as a percentage of the value obtained in the absence of deliberately added ions (control). From the results presented in Fig. 9b, it is clear that the most significant enhancements were from Ca^{2+} and Mg^{2+}. This may be due to the formation of ternary complexes during the charge transfer process. The enhancement effect on the electrocatalytic current for NADH oxidation due to the presence of Ca^{2+} and Mg^{2+} ions was concentration dependent. In case of Ca^{2+} and Mg^{2+}, the maximum effects were observed at a concentration of 10 mM. As the concentration of Ca^{2+} and Mg^{2+} are more than 10 mM, a decreased activity coefficient and adsorption of NADH is observed because of the increase ionic strength [17, 47].

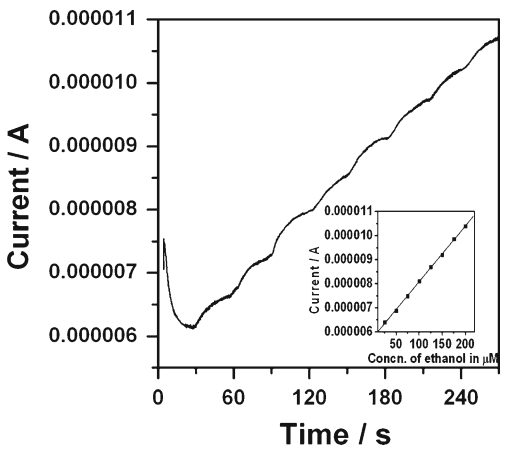

Fig. 10 Chronoamperometric response for the sensing of ethanol by Gr/(PDDA/PSS-[MWCNTs-NH_3^+-graphene-COO^-]$_5$)-ADH electrode at +0.1 V in phosphate buffer solution containing 3.0 mM NAD^+. *Inset*: plot of ethanol vs. catalytic peak current

Constant amperometric determination of ethanol at Gr/(PDDA/PSS-[MWCNTs-NH_3^+-graphene-COO^-]$_5$)-ADH electrode

An ethanol biosensor was developed using Gr/(PDDA/PSS-[MWCNTs-NH_3^+-graphene-COO^-]$_5$) and ADH. The enzyme was cast on the modified electrode and allowed to dry. A steady state amperometric response of Gr/(PDDA/PSS-[MWCNTs-NH_3^+-graphene-COO^-]$_5$)-ADH electrode to the addition of ethanol aliquots to stirred phosphate buffer solution (pH 7.0) in the presence of cofactor NAD^+ at an applied potential of +0.1 V is shown in Fig. 10. Upon addition of an aliquot of ethanol, the oxidation current increased steeply and attained stable value within 5 s, indicating a fast response at the electrode. The electrode responds linearly to ethanol concentration over the range of 25–200 μM with a good sensitivity of 82.5 nA cm^{-2} μM^{-1}. The stability of the enzyme modified electrode was investigated after 5 days, and the response current was still retained at 92 % of the initial response. This implies that the Gr/(PDDA/PSS-[MWCNTs-NH_3^+-graphene-COO^-]$_5$) electrode was efficient for retaining the bioactivity of ADH.

Conclusion

In this work, the electrocatalytic oxidation of NADH at Gr/(PDDA/PSS-[MWCNTs-NH_3^+-graphene-COO^-]$_5$) electrode has been investigated. An overpotential diminution of 0.6 V is achieved at the modified electrode at pH 7.0 with higher electron transfer kinetics. The electrochemical oxidation of NADH is a diffusion controlled process. The modified electrode also offers stable amperometric detection of NADH at a lower applied potential of +0.07 V with a linear range of 25–250 μM and detection limit of 0.1 μM. The modified electrode showed diminished response from its interferences, and the surface fouling was not observed during voltammetric and amperometric measurement of NADH. A biosensor was developed by immobilizing alcohol dehydrogenase enzyme on to the modified electrode to detect ethanol.

Acknowledgments The authors gratefully thank Sri. A.V.S. Murthy, honorary secretary of Rashtreeya Sikshana Samiti Trust, Bangalore and Dr. P. Yashoda, Principal, S.S.M.R.V. Degree College, Bangalore for their continuous support and encouragement. S. Prasanna Kumar personally thank Fr. Roshan Lobo, Principal, St. Joseph's Pre-University College, Bangalore for his support and encouragement.

References

1. Radoi A, Compagone D (2009) Recent advances in NADH electrochemical sensing design. Bioelectrochemistry 76:126–134
2. Ge B, Tan Y, Xie Q, Ma M, Yao S (2009) Preparation of chitosan-dopamine-multiwalled carbon nanotubes nanocomposite for electrocatalytic oxidation and sensitive electroanalysis of NADH. Sensors Actuator B 137:547–554
3. Maroneze CM, Arenas LT, Luz RCS, Benvenutti EV, Landers R, Gushikem Y (2008) Meldola blue immobilized on a new SiO2/TiO2/Graphite composite for electrocatalytic oxidation of NADH. Electrochim Acta 53:4167–4175
4. Vasilescu A, Andreescu S, Bala C, Litescu SC, Noguer T, Marty JL (2003) Screen-printed electrodes with electropolymerized meldola blue as versatile detectors in biosensors. Biosens Bioelectron 18:781–790
5. Gurban AM, Noguer T, Bala C, Rotariu L (2008) Improvement of NADH detection using prussian blue modified screen-printed electrodes and different strategies of immobilization. Sensors Actuators B 128:536–544
6. Ramesh P, Sivakumar P, Sampath S (2003) Phenoxazine functionalized exfoliated graphite based electrodes for NADH oxidation and ethanol biosensing. Electroanalysis 15:1850–1858
7. Gligor D, Dilgin Y, Popescu LC, Gorton L (2009) Poly-phenothiazine derivative modified glassy carbon electrode for NADH electrocatalytic oxidation. Electrochim Acta 54:3124–3128
8. Ogino Y, Takagi K, Kano K, Ikeda T (1995) Reactions between diaphorase and quinone compounds in bioelectrocatalytic redox reactions of NADH and NAD^+. J Electroanal Chem 396:517–524
9. Ramesh P, Sampath S (2000) A binderless, bulk –modified, renewable surface amperometric sensor for NADH and ethanol. Anal Chem 72:3369–3373
10. Matsue T, Suda M, Uchida I (1987) Electrocatalytic oxidation of NADH by ferrocene derivatives and the influence of cyclodextrin complexation. J Electroanal Chem 234:163–173
11. Serban S, Murr NE (2004) Synergetic effect for NADH oxidation of ferrocene and zeolite in modified carbon paste electrodes. New approach for dehydrogenase based biosensors. Biosens Bioelectron 20:161–166
12. Silva FDADS, Lopes CB, Costa EDO, Lima PR, Kubota LT, Oliveria M, Goulart F (2010) Poly-xanthurenic acid as an efficient mediator for the electrocatalytic oxidation of NADH. Electrochem Commun 12:450–454
13. Mu S, Zhang Y, Zhai J (2009) Electrocatalysis of NADH oxidation by nanostructured Poly(aniline-co-2-amino-4-hydroxybenzenesulphonic acid) and experimental evidence for the catalytic mechanism. Electrochem Commun 11:1960–1963
14. Balamurugan A, Chen SM (2008) Voltammetric oxidation of NADH at phenyl azo aniline/PEDOT modified electrode. Sensors Actuators B 129:850–858
15. Manesh KM, Santosh P, Gopalan A, Lee KP (2008) Electrocatalytic oxidation of NADH at gold nanoparticles loaded poly(3,4-ethylenedioxythiophene)-poly(styrene sulfonic acid) film modified electrode and integration of alcohol dehydrogenase for alcohol sensing. Talanta 75:1307–1314
16. Mano N, Kuhn A (1999) Immobilized nitro-fluorenone derivatives as electrocatalysts for NADH oxidation. J Electroanal Chem 477:79–88
17. Mano N, Kuhn A (1999) Ca^{2+} enhanced electrocatalytic oxidation of NADH by immobilized nitro-flurenones. Electrochem Commun 1:497–501
18. Banks C, Compton RG (2005) Exploring the electrocatalytic sites of carbon nanotubes for NADH detection: an edge plane pyrolytic graphite electrode study. Analyst 130:1232–1239
19. Wooten M, Gorski W (2010) Facilitation of NADH electro-oxidation at treated carbon nanotubes. Anal Chem 82:1299–1304
20. Yang DW, Liu HH (2009) Poly(brilliant cresyl blue)-carbon nanotubes modified electrodes for determination of NADH and fabrication of ethanol dehydrogenase-based biosensor. Biosens Bioelectron 25:733–738

21. Luz RDCS, Damos FS, Tanaka AA, Kuboto LT, Gushikem Y (2008) Electrocatalytic activity of 2, 3, 5, 6-tetrachloro-1, 4-benzoquinone/multi-walled carbon nanotubes immobilized on edge plane pyrolitic graphite electrode for NADH oxidation. Electrochim Acta 53:4706–4714
22. Wang Y, Li Y, Tang L, Lu J, Li J (2009) Application of graphene-modified electrode for selective detection of dopamine. Electrochem Commun 11:889–892
23. Shan C, Yang H, Han D, Zhang Q, Ivaska A, Niu L (2010) Electrochemical determination of NADH and ethanol based on ionic liquid-functionalized graphene. Biosens Bioelectron 25:1504–1508
24. Kang XH, Wang J, Wu H, Aksay I, Liu J, Lin Y (2009) Glucose oxidase-graphene-chitosan modified electrode for direct electrochemistry and glucose sensing. Biosens Bioelectron 25:901–905
25. Shan C, Yang H, Han D, Zhang Q, Ivaska A, Niu L (2010) Graphene/ AuNPs/ chitosan nanocomposite film for glucose biosensing. Biosens Bioelectron 25:1070–1074
26. Zheng H, Okada H, Nojima S, Suye SI, Hori T (2004) Layer-by-layer assembly of enzymes and polymerized mediator on electrode surface by electrostatic adsorption. Sci Technol Adv Mater 5:371–376
27. Nethravathi C, Rajamathi M (2008) Chemically modified graphene sheets produced by the solvothermal reduction of colloidal dispersion of graphite oxide. Carbon 46:1994–1998
28. Su CY, Xu Y, Zhang W, Zhao J, Liu A, Tang X, Tsai CH, Huang Y, Li LJ (2010) Highly efficient restoration of graphitic structure in graphene oxide using alcohol vapors. ACS Nano 4:5285–5292
29. Gilje S, Han S, Wang M, Wang KL, Kaner RB (2007) A chemical route to graphene for device applications. Nano Lett 7:3394–3398
30. Prasanna Kumar S, Manjunatha R, Nethravathi C, Suresh GS, Rajamathi M, Venkatesha TV (2011) Electrocatalytic oxidation of NADH on functionalized graphene modified graphite electrode. Electroanalysis 23:842–849
31. Woo Lee S, Kim BS, Chen S, Shao-Horn Y, Hammond PT (2009) Layer-by-Layer assembly of all carbon nanotube ultrathin films for electrochemical applications. J Am Chem Soc 131:671–679
32. Huang KJ, Niu DJ, Sun JY, Han CH, Wu ZW, Li YL, Xiong XQ (2011) Novel electrochemical sensor based on functinalized graphene for simultaneous determination of adenine and guanine in DNA. Colloids Surf B Biointerfaces 82:543–549
33. Liu A, Wei M, Honma I, Zhou H (2006) Biosensing properties of titanate-nanotube films: selective detection of dopamine in the presence of ascorbate and uric acid. Adv Funct Mater 16:371–376
34. Meng L, Wu P, Chen G, Cai C, Sun Y, Yuan Z (2009) Low potential detection of glutamate based on the electrocatalytic oxidation of NADH at thionine/single-walled carbon nanotubes composite modified electrode. Biosens Bioelectron 24:1751–1756
35. Zeng J, Wei W, Wu L, Liu X, Liu K, Li Y (2006) Fabrication of poly(toluidine blue O)/Carbon Nanotube composite nanowires and its stable low-potential detection of NADH. J Electroanal Chem 595:152–160
36. Jensen MA, Elving PJ (1978) Oxidation of l, 4 NADH at a glassy carbon electrode: Effects of pH, lewis acids and adsorption. Bioelectrochem Bioenerg 5:526–534
37. Prieto-Simon B, Fabregas E (2006) New redox mediator-modified polysulfone composite films for the development of dehydrogenase-based biosensors. Biosens Bioelectron 22:131–137
38. Li M, Jing L (2007) Electrochemical behavior of acetaminophen and its detection on the PANI-MWCNTs composite modified electrode. Electrochim Acta 52:3250–3257
39. Wang C, Li C, Wang F, Wang C (2006) Covalent modification of glassy carbon electrode with L-Cysteine for the determination of acetoaminophen. Microchim Acta 155:365–371
40. Yang M, Qu F, Li Y, He Y, Shen G, Yu R (2007) Direct electrochemistry of hemoglobin in gold nanowire array. Biosens Bioelectron 23:414–420
41. Deng C, Chen J, Chen X, Xiao C, Nie Z, Yao S (2008) Boron-doped carbon nanotubes modified electrode for electroanalysis of NADH. Electrochem Commun 10:907–909
42. Salami A, Hallaj R, Ghadermazi M (2005) Modification of carbon ceramic electrode prepared with sol-gel technique by thin film of chlorogenic acid: application to amperometric detection of NADH. Talanta 65:888–894
43. Dai Z, Lu G, Bao J, Huang X, Huangxian (2007) Low potential detection of NADH at titanium-containing MCM-41 modified glassy carbon electrode. Electroanalysis 19:604–607
44. Rao TN, Yagi I, Miwa T, Tryk DA, Fujishima A (1999) Electrochemical oxidation of NADH at highly boron-doped diamond electrodes. Anal Chem 71:2506–2511
45. Yemini M, Reches M, Gazit E, Rishpon J (2005) Peptide nanotube-modified electrodes for enzyme-biosensor applications. Anal Chem 77:5155–5159
46. Vasantha VS, Chen SM (2006) Synergistic effect of catechin-immobilized poly (3,4- ethylenedioxythiophene)-modified electrode on electrocatalysis of NADH in the presence of ascorbic acid and uric acid. Electrochim Acta 52:665–674
47. Pariente F, Tobalina F, Moreno G, Hernandez L, Lorenzo E, Abruna HD (1997) Mechanistic studies of the electrocatalytic oxidation of NADH and ascorbate at glassy carbon electrodes modified with electrodeposited films derived from 3, 4- dihydroxybenzaldehyde. Anal Chem 69:4065–4075